Polymer 55 (2014) 2422–2431

Contents lists available at ScienceDirect

Polymer

journal homepage: www.elsevier.com/locate/polymer

Supercritical CO_2 and polycarbonate based nanocomposites: A critical issue for foaming

Laure Monnereau [a], Laetitia Urbanczyk [b], Jean-Michel Thomassin [b], Michaël Alexandre [b], Christine Jérôme [b], Isabelle Huynen [c], Christian Bailly [c], Christophe Detrembleur [b,*]

[a] Institute of Organic Chemistry, KIT-Campus South, Fritz-Haber Weg 6, 76131 Karlsruhe, Germany
[b] Center for Education and Research on Macromolecules (CERM), University of Liège, Building B6a, 4000 Liège, Belgium
[c] Research Center in Micro and Nanoscopic Materials and Electronic Devices, CeRMiN, Université Catholique de Louvain, 1348 Louvain-la-Neuve, Belgium

ARTICLE INFO

Article history:
Received 19 December 2013
Received in revised form
11 March 2014
Accepted 20 March 2014
Available online 28 March 2014

Keywords:
Polycarbonate
Carbon nanotubes
Foaming

ABSTRACT

Supercritical carbon dioxide readily induced foaming of various polymers. In that context, supercritical CO_2 was applied to carbon nanotubes based polycarbonate nanocomposites to ensure their foaming. Surprisingly, efficient foaming only occurs when low pressure is applied while at high pressure, no expansion of the samples was observed. This is related to the ability of supercritical carbon dioxide to induce crystallization of amorphous polycarbonate. Moreover, this behaviour is amplified by the presence of carbon nanotubes that act as nucleating agents for crystals birth. The thermal behaviour of the composites was analysed by DSC and DMA and was related to the foaming observations. The uniformity of the cellular structure was analysed by scanning electron microscopy (SEM). By saturating the polycarbonate nanocomposites reinforced with 1 wt% of MWNTs at 100 bar and 100 °C during 16 h, microcellular foams were generated, with a density of 0.62, a cell size ranging from 0.6 to 4 μm, and a cellular density of 4.1×10^{11} cells cm^{-3}. The high ability of these polymeric foams to absorb electromagnetic radiation was demonstrated at low MWNT content as the result of the high affinity of the polycarbonate matrix for MWNTs, and therefore to the good MWNTs dispersion.

1. Introduction

Studies of the structure–property relationships of multicomponent polymer/inorganic additives systems have recently gained in interest due to their wide technological applications. Among the inorganic nanocomposites, carbon nanotubes have attracting significant attention as a new class of nanoadditives that can improve the performance properties of polymeric matrices. Once combined to a polymer, they confer greatly improved physical [1] and mechanical properties or new functional properties at relatively low nanofiller loading levels in comparison with conventional microcomposites, which commend them for use in high performance technology [2,3]. Numerous studies on the preparation, structure and properties of multi-walled carbon nanotubes (MWNTs) based nanocomposites have been carried out [4]. Most of these systems are characterized by scarcely miscible constituents forming multiphase materials whose properties are strongly affected by the mode of dispersion, size, and orientation of the nanofiller. Polycarbonate (PC) has several advantages among the other polymers as it exhibits high thermal stability, a high toughness, transparency, and high impact resistance. It is mostly used in the preparation of glasses or CD/DVDs, in various transparent constructions, household devices, or protection equipment, for instance as constituent of motorbike crash helmet [5]. Few works on MWNTs/PC nanocomposites prepared through simple melt-extrusion have already been reported [6–15]. The combination of PC with carbon nanotubes results in a material exhibiting electrical conductive properties with a high impact strength, modulus, heat resistance, whereas pure polymer are usually electrical insulators.

Foaming of these polymer/CNTs nanocomposites can be advantageous for many applications such as in electromagnetic interference (EMI) shielding devices. Together with a gain of weight, the foaming can indeed decrease the permittivity of the generating material by creating voids inside the polymeric matrix. This characteristic is of first importance in the context of designing high performance EMI absorbers [16]. The reflection on the surface

* Corresponding author. Tel.: +32 43663465; fax: +32 43663497.
E-mail address: christophe.detrembleur@ulg.ac.be (C. Detrembleur).

http://dx.doi.org/10.1016/j.polymer.2014.03.035
0032-3861/

of the materials is indeed proportional to the permittivity of the materials.

In this work, supercritical CO_2 ($scCO_2$) is used to expand the PC/MWNTs nanocomposites and to provide well-defined nanocomposite foams. Currently, only a little number of study have been reported on that topic, due to the challenge that represents the effective foaming of polycarbonate [17–22]. We investigate the microstructure of melt-blended samples of PC with MWNTs by transmission electron microscopy (TEM) and rheology. The presence of crystallites in polycarbonate has a strong impact on the foaming behaviour. Consequently, efforts were made at rationalizing the effect of $scCO_2$ infusion and carbon nanotubes content on the crystallization process that occurs under the experimental conditions of saturation. The final properties of the impregnated nanocomposites were investigated by dynamic scanning calorimetry (DSC) and dynamic mechanical analysis (DMA). Finally, the morphology of the resulting foams was characterized by SEM and their performances as EMI shielding materials were evaluated. To the best of our knowledge, this is the first reported systematic study concerning the effect of multi-walled carbon nanotubes in the supercritical CO_2-induced crystallization of reinforced polycarbonate.

2. Materials and methods

2.1. Nanocomposites preparation

Polycarbonate (PC) under the trade name Makrolon® 2805A (from Bayer, Germany), and multi-walled carbon nanotubes thin (MWNTs) NC7000 (from Nanocyl™ S.A., Belgium, produced via the Catalytic Carbon Vapour Deposition (CCVD) process, with an average outer diameter of 9.5 nm, and an average length of 1.5 μm) were used as received. The Makrolon grade developed by Bayer is obtained by transesterification of bisphenol A with a diaryl carbonate in the melt phase [23], and was dried before use in a vacuum oven at 100 °C during at least 16 h to minimize the possibility of hydrolysis during the mixing. PC-MWNTs blends, containing 0, 0.25, 0.5, 1 and 2 weight per cent (wt%) of MWNTs, respectively, were prepared by extrusion in a counter rotating twin-screw internal mixer (Brabender®) operating at 60 r.p.m. and 250 °C during 5 min. The pure polymer and the blends were moulded in the form of 0.75 mm − and 2 mm-thick slabs for DSC-DMA measurements and for foaming experiments, respectively.

2.2. Nanocomposites characterization

MWNTs dispersion was observed with a transmission electron microscope PHILIPS M100 at an accelerating voltage of 100 kV. Thin sections (90 nm) were prepared by ultramicrotomy (ULTRACUT E from REICHERT-JUNG) at −130 °C. Micrographs were analysed by using the megaview GII (Olympus) software.

Dynamic rheological measurements were carried out with an advanced rheometric expansion system (ARES G2) rheometer from TA instruments. Samples (diameter 25 mm, thickness 2 mm) were run at 250 °C with a strain of 1%.

2.3. Foam processing

PC foams have been prepared according to the solid-state foaming process (or two-step process) by saturating polymer slices (40 × 20 × 2 mm) with CO_2 (99,9998%, Air Liquide, Belgium) during 24 h into a stainless steel high pressure autoclave previously flushed with CO_2 once the samples were introduced (Parr instruments, 250 mL). After a quick depressurization (within 30 s), foaming occurred by placing the sample in a hot press at 190 °C during 190 s. Finally, stabilization of the foam structure is performed by cooling down the sample in an ice-water bath.

2.4. Foam characterization

Foam density (ρ_f) is estimated by weighting a foamed sample of known volume, and the foam morphology of the PC/MWNTs nanocomposites is observed by scanning the fracture surface using the field-emission SEM (JEOL JSM-840-A) at an accelerating voltage of 15 kV. The samples are first dived into liquid nitrogen before fracture to avoid a consequent ductile deformation and the fracture surface is coated with a thin layer of platinum (30 nm). Image analysis is manually performed on the basis of SEM pictures by measuring the size of at least 100 cells. Cell density (N_{cell}) relative to unfoamed polymer is deduced from the SEM picture [24].

The density of multi-walled carbon nanotubes can be calculated by the equation (1):

$$\rho_{CNTs} = \frac{\rho_g\left(d^2 - d_i^2\right)}{d^2} \quad (1)$$

where ρ_g is the density of fully dense graphite which is equal to 2.25 g/cm^3, d and d_i are outer and inner diameter of carbon nanotube, respectively. The theory of percolation threshold is considered as a volumetric phenomenon. Therefore, by knowing the ρ_{CNTs}, the weight percentage (wt%) of MWNTs can be transformed into volume percentage (Vol%) of MWNTs.

2.5. Thermal behaviour investigation

The glass transition temperature (T_g) and the melting temperature (T_m) of each sample were determined with a TA Q100 DSC thermal analyser calibrated with indium. Samples were encapsulated in aluminium pans and the following cycle was used: heating from 40 °C to 260 °C at 10 °C min^{-1} (run I) then cooling to 40 °C at 20 °C min^{-1}, and heating from 40 °C to 260 °C (run II) under a dry nitrogen atmosphere. Melting temperatures and relevant enthalpies of PC and PC/MWNTs in the various samples were determined from the maxima and the areas of DSC peaks. The saturated samples were first desorbed at room temperature during several days before being analysed by DSC to avoid the presence of CO_2 desorption peak in the thermogram.

Dynamic mechanical properties of samples were analysed using a dynamic mechanical analysis (DMA; Q800, TA Instruments). Rectangular specimens, 40 mm in length, 20 mm in width, and 0.75 mm in thickness were prepared. The measurements were taken in 3-points bending mode at a frequency of 1 Hz and strain of 0.1%. Samples were previously cooled from room to liquid nitrogen temperature, at a cooling rate of about −10 °C min^{-1}, and subsequently heated up to 300 °C at 1 °C min^{-1}. The storage modulus (E′) and damping factor (tan δ) of the samples were measured as a function of temperature.

2.6. Electromagnetic characterization

Electrical properties of MWNT/polymer composites were measured with a Wiltron 360B Vector Network Analyzer (VNA) in a wideband frequency range from 40 MHz to 40 GHz. Complex dielectric constant and conductivity were extracted from the VNA transmission and reflection measurements, which also yielded the absorbed power. Solid samples were characterized in a microstrip line topology, while foamed samples were placed in a rectangular waveguide configuration. The two techniques are explained and illustrated in Ref. [70].

3. Results and discussion

3.1. Nanocomposites morphology

In the polymeric domain, a classical way to confer additional properties upon a targeted matrix consists in incorporating nanofillers, as carbon black, carbon fibres or carbon nanotubes. This subject has been extensively reviewed [4] and in the context of elaborating conductive materials, carbon nanotubes established themselves as leader, as they present unique electrical and mechanical properties and high aspect ratio [25,26]. As these nanofillers are usually considered as expensive additives, this latter characteristic has a certain economical feature as low concentration of fillers can be therefore incorporated, preventing from an eventual increase of the cost of the resulting material. Dispersion of the nanofillers is of crucial interest to transfer the expected properties to the polymeric matrix. The choice of dispersive techniques is wide-ranging, as dilution of masterbatch, co-precipitation, ultrasonification, or melt-blending [4,15,27]. In this study, the dispersion of carbon nanotubes into polycarbonate matrix is carried out by melt-blending at 250 °C and analysed by transmission electronic microscopy. According to the TEM picture of PC reinforced with 1 wt% of multi-walled carbon nanotubes (MWNTs), the fillers are well-dispersed into the polycarbonate matrix, no agglomeration being observed (Fig. 1).

We have also investigated the behaviour of PC nanocomposites in terms of melt-state oscillatory rheology at 250 °C (Fig. 2). Indeed an effective dispersion of the carbon nanotubes influences the rheological behaviour of PC as these latter increased the storage modulus (G′). At low frequency range, the pure PC has a liquid-like behaviour, G′ being dependent with the frequency. With addition of a minimal content of 0.25 wt% of MWNTs, the storage modulus of PC increases rapidly and becomes essentially independent of frequency. This change indicates a transition from a liquid-like to a solid-like viscoelastic behaviour [28], the storage modulus being sensitive to the percolation of nanofillers in the low-frequency range. This behaviour results from the building-up of a carbon nanotubes network, which restrains the long-range motion of PC chains. The percolation threshold is thus reached when G′ showed a plateau at low frequency range, which is already the case with the PC/0.25 wt% MWNT samples, showing an adequate dispersion of the MWNTs into the polycarbonate matrix.

The performances of these nanocomposites have also been investigated in terms of electrical conductivity (Fig. 3). As expected from dielectric materials, the PC samples appear to be poor conductive materials since the value of σ remains low whatever the frequency studied. For the nanocomposites filled with MWNTs, the conductivity increases with the frequency, the electrical properties of the materials coming from the incorporation of the conducting fillers. When EMI shielding applications are targeted, the material

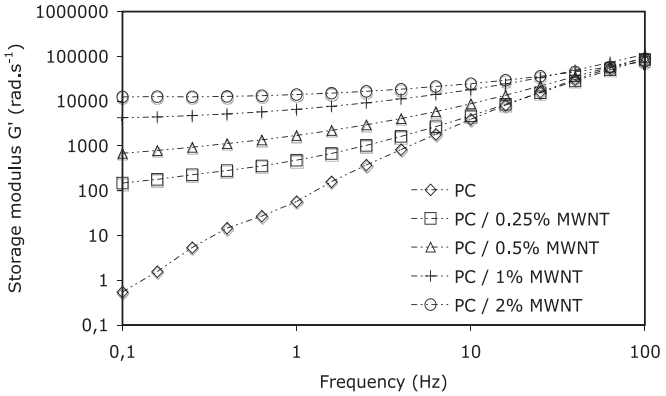

Fig. 2. Storage modulus as a function of frequency for PC and PC nanocomposites.

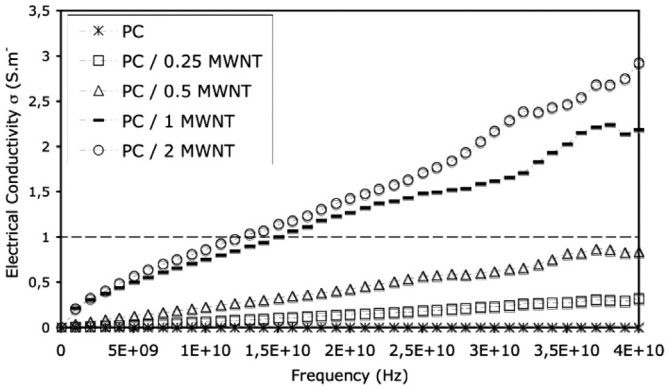

Fig. 3. Electrical conductivity as a function of frequency for PC and PC nanocomposites.

must present a conductivity higher than 1 S m^{-1} in order to develop satisfactory EMI performances [29] This objective is reached for PC containing 1 and 2 wt% MWNT in the frequency range of 15–40 GHz (Fig. 3). Therefore, the foaming studies discussed below will focus on PC nanocomposites preloaded with 1 wt% and 2 wt% of MWNTs.

3.2. Foaming of the MWNT/PC nanocomposites

Polycarbonate is one of the most challenging polymer to foam because of its intrinsic properties in terms of mechanical strength. Indeed, this polymeric matrix is characterized by a high viscosity, and the addition of MWNTs increases this trend, as testified by the augmentation of the storage modulus with the addition of MWNTs (Fig. 2). Several processes have been currently employed to lead to

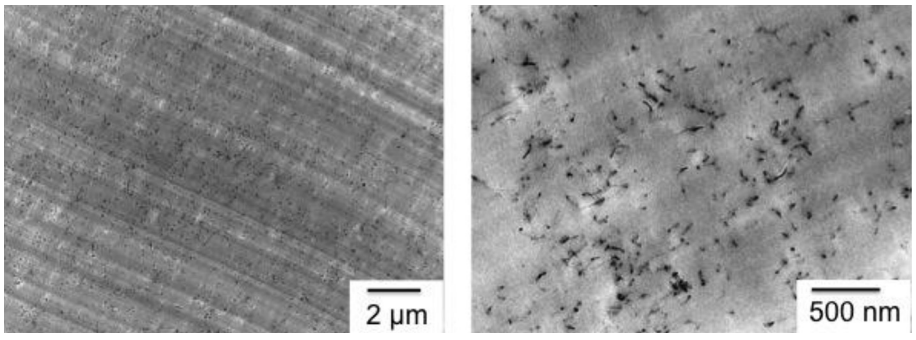

Fig. 1. TEM micrographs of PC/1 wt% MWNTs.

sufficiently expanded polycarbonate, the best route being obtained by the use of physical blowing agent (MuCell™ process, which mainly operates with N_2) [30,31]. In this study, we used $scCO_2$ as foaming agent to create foam with no residual additives. Supercritical fluids have been extensively studied as new alternative blowing agents, as they present a certain number of positive aspects; their use prevent from the presence of residual blowing agent into the polymeric matrix once foaming has occurred, and they have no environmental impact. Since supercritical CO_2 has a zero depletion order, and since its critical parameters are easily achieved (Pc = 73.8 °C and Tc = 31.1 °C), $scCO_2$ has established itself as a leader in the large area of physical blowing agents [32,33].

Foaming with $scCO_2$ is realized in a high-pressure autoclave by saturating the sample during the desired period of time followed by expansion of the material. As polycarbonate possesses a high T_g, the solid-state foaming process was envisaged. In this method, the depressurization of the autoclave is performed at moderate temperature where the polymer is in the glassy state and too rigid to allow cell growth, the expansion step being performed during a subsequent heating at a higher temperature. To reach the optimal foaming conditions, the adequate pressure is determined by exploring the range between 75 and 250 bar, the saturation temperature has been arbitrary set to 100 °C and the expansion of the sample occurred in a second step in a hot press at 190 °C during 190 s (Table 1). In this process, only two conditions lead to an effective foaming of the material loaded with 2 wt% of MWNTs, with a minimal density of 0.65 when saturating the sample at 100 bar (Table 1, entry 1). Operating between 150 and 250 bar prevents from any foaming (Table 1, entries 3–5) contrary to what is expected from the nucleation growth theory forecast [34,35]. Indeed, saturating a sample at high pressure assured a higher penetration of CO_2 molecules into the polymeric matrix. It also induced a higher depressurization rate, both effects usually lead to a better expansion of the sample thank to the increased CO_2 content. To the light of these unexpected results, we have investigated deeper the $scCO_2$/PC/MWNTs system in terms of thermal and mechanical behaviour before continuing to study the foaming of PC nanocomposites.

3.3. Thermal behaviour of PC/MWNTs nanocomposites saturated with $scCO_2$

We first characterized the supercritical CO_2/PC/2 wt% MWNTs system by DSC measurements in function of the saturation pressure (Fig. 4). The nanocomposites are saturated at the desired pressure during 24 h at 100 °C. The pressure is quickly released (time inferior to 10 s, volume of the autoclave: 12 mL), and the samples are desorbed at room temperature during 7 days before being analysed to avoid peaks resulting from the desorption of CO_2. The nanocomposites present a variation in their thermal behaviour according to the applied saturation pressure (each conditions in Fig. 4 are shifted vertically for clarity). At 75 bar and 100 bar, the nanocomposites have an amorphous behaviour, with a glass transition temperature appearing at 136 °C (*cf.* Table 2). When applying a pressure of 150 bar, the PC reinforced with 2 wt% MWNTs showed two melting endotherms additionally to the glass transition temperature. This phenomenon is amplified when the saturation pressure is increased to 200 and 250 bar, the endothermic peaks presenting a larger area (*cf.* $\Delta_{f,n}$ values in Table 2). The apparition of this crystallization is relied to the plastification effect of supercritical CO_2 [36–41]. Indeed the polycarbonate chains tend to form thermodynamically stable crystallites. However, the poor mobility of their chains extremely slow down their formation and they only appeared during long annealing treatment at temperatures superior to 180 °C [42]. The presence of CO_2 impregnated within PC significantly increased the mobility of the chains and consequently favours the formation of crystallites. CO_2-induced crystallization was previously reported for several neat polymers such as poly(ethylene terephthalate) [43,44], polypropylene [45], PEEK (tert-butyl-poly(ether ether ketone)) derivatives [46], polylactide, [47] Poly(VinyliDeneFluoride)/Poly(Methyl MethAcrylate) blends [43,48], but also for pure PC [45,49,50], and according to our observations, the behaviour of the MWNTs nanocomposites follows this trend. For a sake of comparison, the PC based nanocomposites are heated at 100 °C during 24 h without any impregnation with $scCO_2$. In that case (not represented on Fig. 4), the samples presented a complete amorphous behaviour.

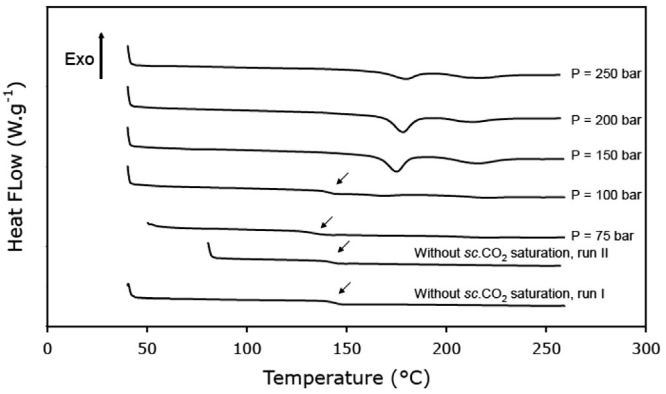

Fig. 4. Thermal behaviour of PC/2% MWNT nanocomposites saturated at 100 °C in function of saturation pressure of $scCO_2$. The black arrow indicates the presence of T_g.

According to Fig. 4, the CO_2-induced crystallization of MWNTs nanocomposites appears as two melting endotherms. To quantify and rationalize this behaviour, the degree of crystallinity of the nanocomposites was calculated according to equation (2) using the heat of fusion per gram of PC determined from the DSC measurements and the heat of fusion corresponding to 100% crystalline PC (ΔH_f° = 109.7 J g^{-1} ΔH_f° of bisphenol A polycarbonate) [51].

$$P = \Delta H_f(\text{sample}) \Big/ \Delta H_f^\circ \qquad (2)$$

The melting point (T_m), heat of fusion (ΔH_m) and the percent of crystallinity ($\%_{cryst.}$) obtained from the DSC thermogram are listed in Table 2. At a pressure of 75 bar, CO_2 has only an effect on the glass transition temperature of the nanocomposites which is decreased from 144 °C to 136 °C. (Table 2, entries 1 and 2). When the nanocomposite is saturated at 100 bar, the crystallization process begins and the glass transition temperature increased again due to the presence of crystalline region that restrains the chain mobility. When the pressure of $scCO_2$ increases again, the amount of CO_2 sorbed is incremented, thereby enhancing the degree of crystallinity of the polymer whereas the glass transition temperature is

Table 1
Effect of saturation pressure on PC/2 wt% MWNT foam morphology.[a]

Entry	Pressure (bar)	$\%CO_2$ (wt%)	d_f (g/cm^3)	N_{cells} (cells cm^{-3})	Size of cells (μm)
1	75	3.0	0.82	5.1×10^8	2.4–30
2	100	6.7	0.65	5.0×10^{11}	0.6–8.5
3	150	10.1	1.20	none foaming	
4	200	10.5	1.20	none foaming	
5	250	11.2	1.20	none foaming	

[a] The runs were performed at 100 °C during 24 h. Density is determined by measuring the sample dimensions and weight. The cellular density N_{cells} and the size of the cells are determined by image analysis on the basis of SEM pictures.

Table 2
Crystallization and Melting behaviours of PC/2 wt% MWNTs nanocomposites saturated at a temperature of 100 °C in function of the saturation pressure of $scCO_2$.[a]

Entry	P_{sat}	$\%CO_2$ sorbed	T_g	T_{m1} T_{m2}	$\Delta H_{f1,n}$ $\Delta H_{f2,n}$	$\%_1$ $\%_2$	Crystallinity
1	/	/	144	/	/	/	
2	75	4.6	136	/	/	/	
3	100	6.9	140	168	0.9	0.8	
				/	/	/	
4	150	6.5	*nd*	175	11.5	10.5	
				215	8.3	7.5	
5	200	7.0	*nd*	178	11.9	10.8	
				213	5.2	4.8	
6	250	6.8	*nd*	179	21.1	19.3	
				216			

nd means not detected.
[a] The runs were performed at 100 °C during 24 h. Temperature, enthalpy and crystallinity are expressed in bar, joules per gram and percent, respectively.

Table 3
Crystallization and Melting behaviours of PC/2 wt % MWNTs nanocomposites saturated at a pressure of 75 bar of $scCO_2$ in function of the saturation temperature.

T_{sat}	$\%CO_2$ sorbed	T_g	T_{m1} T_{m2}	$\Delta H_{f1,n}$ $\Delta H_{f2,n}$	$\%_1$ $\%_2$	Crystallinity
/	/	144	/	/	/	
80[a]	5.0	140	/	/	/	
100[a]	4.6	136	/	/	/	
120[a]	4.0	140	/	/	/	
			217	0.9	0.8	
150[a]	1.9	143	178	5.6	5.0	
			214	3.5	3.2	
140[b]	2.3	135	/	/	/	
			216	7.9	7.2	
170[b]	1.7	142	189	5.7	5.2	
			218	4.1	3.7	

[a] The runs were performed at 75 bar during 24 h. Temperature, enthalpy and crystallinity are expressed in bar, joules per gram and percent, respectively.
[b] The runs were performed at 75 bar during 72 h.

maintained close to 139 °C (Table 2, entries 3 and 4). Between 150 and 250 bar, the T_g is not detected in the thermogram. At 250 bar, the melting endotherms begin to merge and a simultaneously integration of the two endotherms is preferred to avoid errors in the value of the degree of crystallization. It raises its maximal value to 19.3%. The larger intensity of the two endotherms in parallel with the augmentation of the amount of CO_2 sorbed correlates to the CO_2-induced crystallization phenomena. These two endotherms were previously interpreted as two melting temperatures, a lower one (T_{m1}) and a higher one (T_{m2}), related to the thermal behaviour of two populations of crystals [52]. The crystals related to Tm_2 are formed during the primary crystals process [53] whereas those of Tm_1 came from the secondary crystallization process.

3.3.1. *Effect of the saturation temperature*

The effect of saturation temperature was also taken into account in this study. We have saturated the samples loaded with 2 wt% of MWNTs at a pressure of 75 bar, pressure at which no melting peak was detected in our previous experiments when the nanocomposites were heated at 100 °C. By varying the saturation temperature from 80 °C to 170 °C, the endotherm peak related to T_{m2} is detected at 140 °C (Fig. 5 and Table 3). By saturating the samples at 150 °C, the second endotherm peak (T_{m1}) appears and the area of the peaks increased with higher temperature, for instance at 170 °C (Table 3). When the temperature increased, the molecular mobility of the polymeric chains is improved, giving the possibility to the system to reorganize itself and leads to the emergence of small crystallites.

According to our previous experiments, high pressure of $scCO_2$ leads to crystallization of PC/2 wt% MWNTs, and an increase in the saturation temperature has also a benefit effect on this phenomena. The nanocomposites are then saturated at 250 bar with an increasing temperature to determine if a conjugated effect of pressure and temperature can be obtained (Fig. 6). Considering the values of percent of crystallinity determined by the DSC measurements, one can conclude that a maximal crystallization of nearby 20% is achieved by saturating the samples at 250 bar and 150 °C for 24 h (Table 4) whereas at 75 bar, the total percent of crystallinity raised a value of 8.2% (Table 3). As a comparison, the crystallization of neat polycarbonate is extremely slow, with a crystallization half-time of 12 days at 190 °C due to the chain rigidity [54].

3.3.2. *Effect of the carbon nanotubes content on crystallinity*

Crystallization in polymers can generally be induced and controlled by several means such as addition of nucleating agents or plasticizers [14,55], thermal annealing [56], pressure [23], solvent vapour [57,58], liquid exposure [59–61], or with the presence of a surfactant [62]. Crystallization of polycarbonate was already achieved in 400 and 200 s by blending with crystalline polymers such as poly(ethylene oxide) but temperature of 140 and 180 °C, respectively, were still needed [63]. These high temperatures are usually required to crystallize polycarbonate, even in the presence of plasticizers. As MWNTs additives substantially changed PC glass transition characteristics, as estimated by DSC, the goal of this work

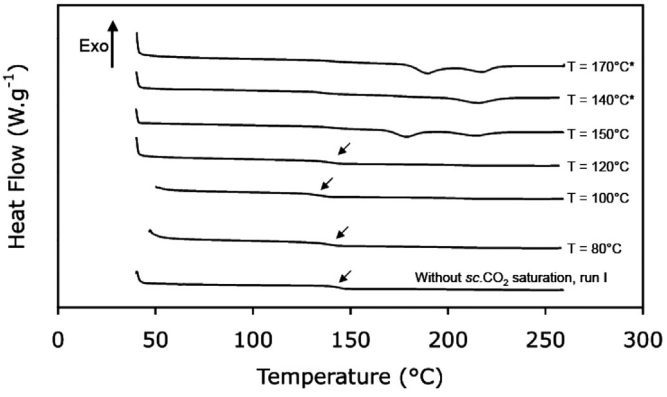

Fig. 5. Thermal behaviour of PC/2 wt% MWNT nanocomposites at 75 bar in function of saturation temperature. The black arrow indicates the presence of T_g. Samples with * were sorbed during 72 h.

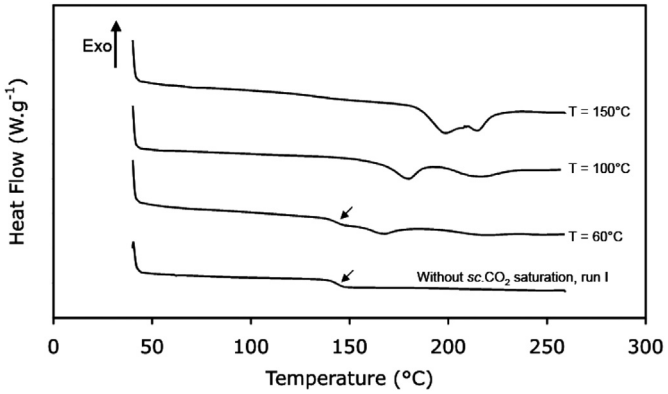

Fig. 6. Thermal behaviour of PC/2 wt% MWNT nanocomposites at 250 bar in function of saturation temperature.

Table 4
Crystallization and Melting behaviours of PC/2 wt% MWNTs nanocomposites saturated at a pressure of 250 bar of $scCO_2$ in function of the saturation temperature.[a]

T_{sat}	$\%CO_2$ sorbed	T_g	T_{m1} T_{m2}	$\Delta H_{f1,n}$ $\Delta H_{f2,n}$	$\%_1$ $\%_2$	Crystallinity
60	11.9	143	/	/	/	
100	6.9	140	168 /	0.9 /	0.8 /	
150	6.8	*nd*	198 215	21.9	19.9	

nd means not detected.
[a] The runs were performed at 250 bar during 24 h. Temperature, enthalpy and crystallinity are expressed in bar, joules per gram and percent, respectively.

is to determine an eventual concomitant effect of the amount of MWNTs in the crystallization phenomena induced by $scCO_2$. Samples loaded with 0.25%, 0.5%, 1% and 2% of nanofillers are consequently prepared and saturated at various pressure and temperature during 24 h and thermally characterized by DSC measurements. Fig. 7a and b presents the percent of crystallinity in function of the saturation temperature and of the saturation pressure, respectively, for each blend. As a general trend, when the temperature of saturation of $scCO_2$ increases, the quantity of CO_2 sorbed in the nanocomposite decreases contrary to the molecular agitation. Although MWNTs does not significantly affect this behaviour, they can also act as germination nodes for crystals birth [64] and their presence consequently increases the percent of crystallinity compared to the neat polymer (Fig. 7a). When the pressure of $scCO_2$ increases, the amount of CO_2 sorbed increases too, leading to higher value of percent of crystallinity (Fig. 7b). At medium pressure, the crystallinity is clearly higher in presence of CNTs which confirms their nucleating effect.

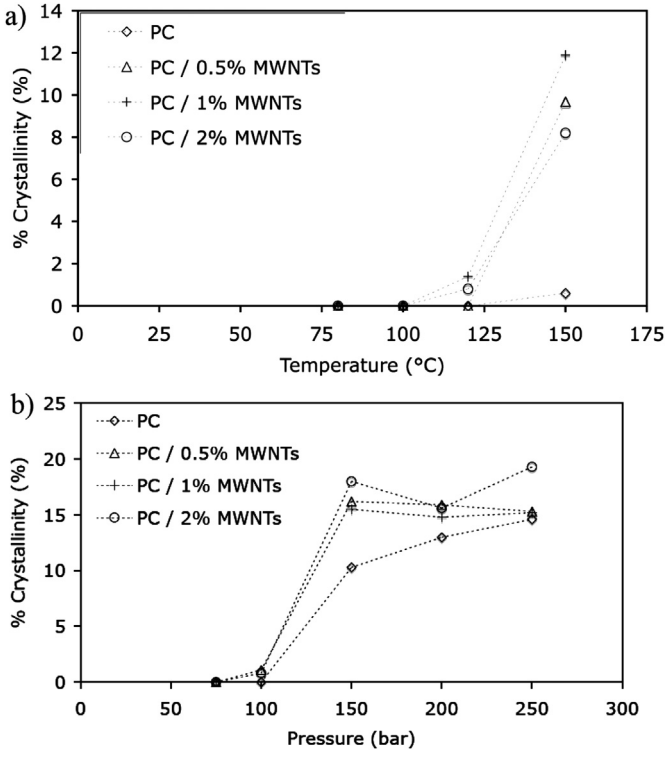

Fig. 7. a) Percent of crystallinity in function of temperature for PC and PC/MWNTs nanocomposites saturated at 75 bar and b) percent of crystallinity in function of saturation pressure for PC and PC/MWNTs nanocomposites saturated at 100 °C.

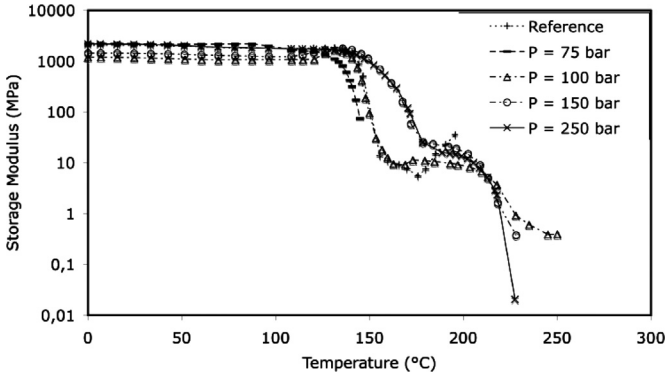

Fig. 8. Temperature dependence of the Young's Modulus E′ for PC/1 wt% MWNTs blends at various saturation pressure.

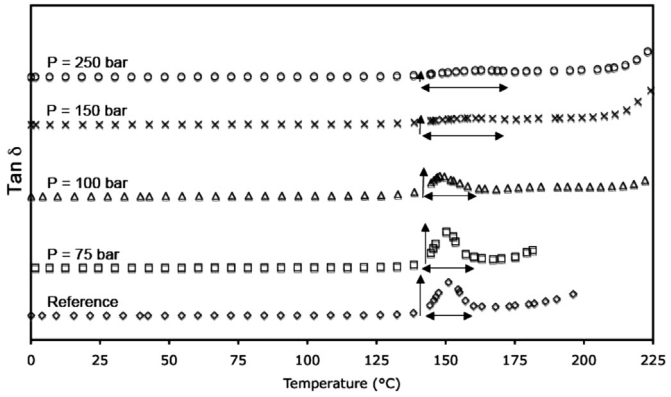

Fig. 9. Temperature dependence of tan δ for PC/1 wt% MWNTs blends at various saturation pressures.

To the light of these experiments, the behaviour of PC/MWNTs samples concerning the foaming experiments can be rationalized in a certain extent with the induced-crystallization phenomena. When the saturation process occurs at high pressure of $scCO_2$, the percent of crystallinity in the nanocomposites increases, which reduced the amount of $scCO_2$ available for the cell growth during the expansion process, and prevents the samples from an important expansion.

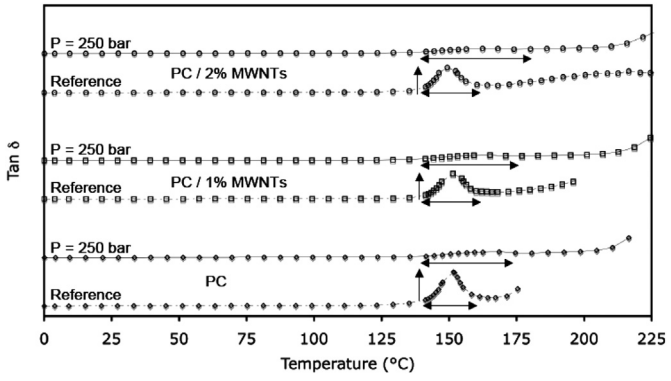

Fig. 10. Temperature dependence of tan δ for PC/MWNTs blends at various compositions saturated at 250 bar of $scCO_2$ and 100 °C (top) and their analogue without exposure to $scCO_2$ (below).

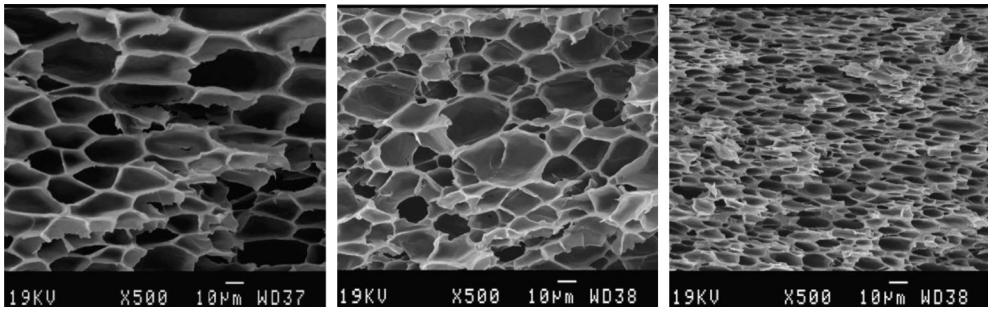

Fig. 11. SEM micrographs of PC (left), PC/1 wt% MWNT (middle) and PC/2 wt% MWNT (right) prepared by solid-state foaming at 75 bar, a saturation temperature of 100 °C, and a foaming temperature of 190 °C.

3.4. Thermal mechanical behaviour of PC/CNT nanocomposites saturated with $scCO_2$

The mechanical properties of the PC/CNT nanocomposites has also been investigated and particularly the effect of the presence of crystalline phases. This study was conducted on PC nanocomposites reinforced with 1 wt% of MWNTs, while the DSC results were conducted on nanocomposites loaded with 2 wt%.

3.4.1. Effect of the $scCO_2$ pressure on the thermal mechanical behaviour of PC/1 wt% MWNTs

The Young's modulus (E′) has been plotted as a function of temperature from 0 to 250 °C for PC/1 wt% MWNTs nanocomposite saturated at 100 °C with various pressures of $scCO_2$ (Fig. 8). Below the glass transition, only slight differences in storage modulus have been observed between the infused composites. These small differences can be explained by small variations of the thickness of the samples due to the CO_2 absorption. In contrast, saturation with CO_2 largely influences the value in storage modulus around and above the glass transition. For instance, when PC/1 wt% MWNTs is saturated at a pressure of 100 bar, the storage modulus reaches a value of 95.2 MPa at 150.0 °C whereas the equivalent sample saturated at 250 bar exhibits a storage modulus of 963.7 MPa. This increase indicates a restraint in the mobility of the polymeric chains due to the increasing percentage of crystallinity.

Fig. 9 shows the shifted dependence of tan δ of PC/1 wt% MWNTs in function of the temperature. For the reference and the sample saturated at 75 bar, the curve shows a maxima which corresponds to the glass transition temperature of the samples, at 150 °C. For the nanocomposites infused at higher pressure, the peak corresponding to T_g becomes broader and is shifted to higher temperature. This can be again correlated with a restriction of the chain mobility due to the increased percent of crystallinity [65].

3.4.2. Effect of the carbon nanotubes on the mechanical behaviour of the PC blends

Fig. 10 shows the variation of tan δ with temperature for neat PC and PC loaded with 1 and 2 wt% of MWNTs, respectively. For each nanocomposite, the curves of tan δ for the infused and the reference samples are shown. Upon addition of MWNTs, the position of the peak maximum in the tan δ curves is slightly shifted towards higher values implying that the MWNTs act as reinforcing fillers.

When neat PC and the composites are exposed to $scCO_2$ treatment, the peak maximum in tan δ decreases in intensity and is shifted to higher temperature in each cases, indicating a restriction of the mobility of the polymeric chains due to the presence of crystal regions. This effect becomes more pronounced when the MWNTs content increases, illustrating again the positive effect of MWNTs on the crystallization of PC chains upon CO_2 treatment.

3.5. Foaming behaviour of PC/MWNTs nanocomposites

Knowing that the crystallization of PC chains has to be avoided to achieve good volume expansion, the maximum temperature (100 °C) and pressure (75 bar) that can be used without the observation of crystallinity in MWNTs filled PC have been chosen to study the influence of MWNTs on the PC foaming.

The SEM micrographs of PC foams containing 0, 1 and 2 wt% MWNTs prepared with the solid-state foaming process are compared in Fig. 11. Foams of neat PC yield to larger cell size in

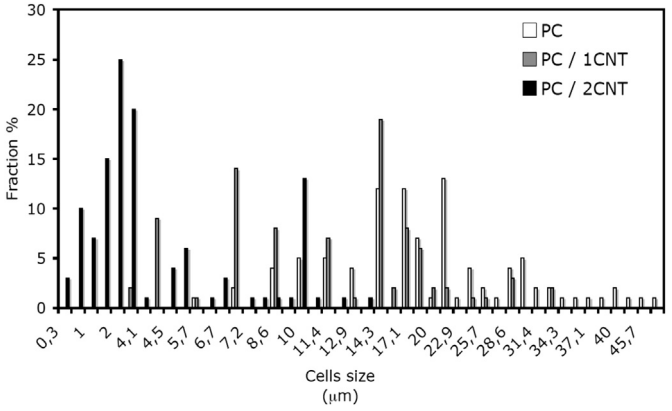

Fig. 12. Cell size distribution of PC/MWNT polymer foams prepared by solid-state foaming at 75 bar, a saturation temperature of 100 °C, and a foaming temperature of 190 °C.

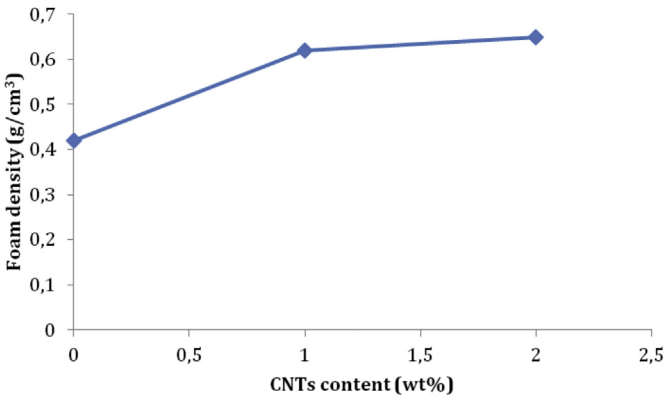

Fig. 13. Foam density as a function of the MWNTs content for foams prepared by solid-state foaming at 75 bar, a saturation temperature of 100 °C, and a foaming temperature of 190 °C.

Table 5
Characteristics of the samples used for EMI shielding characterizations.

Name	Foaming temperature	Foam density	MWNTs content (wt%)	MWNTs content (Vol%)
Foam A	190 °C	0.39	0	
Foam B	190 °C	0.66	2	1.056
Foam C	195 °C	0.56	2	0.896
Foam D	200 °C	0.44	2	0.704
Solid A			0.5	0.5
Solid B			0.75	0.75

contrast to PC/MWNTs nanocomposites, as the result of the cell nucleating ability of carbon nanotubes. The efficiency of MWNTs to generate smaller cells in a higher amount is well-known for other inorganic agents like nanoclays [64,66,67], talc [68], or titanium oxide. [69] They also lead to a more regular morphology, with a narrower cell size range compared to neat polymer. The distribution of the pore size is illustrated in Fig. 12. The presence of MWNTs affords a narrower cell size distribution but limits the expansion volume due to the increase in viscosity imparted by the nanofiller (Fig. 13). The global density remains quite high (around 0.6). Indeed, since the saturation pressure and temperature have to be

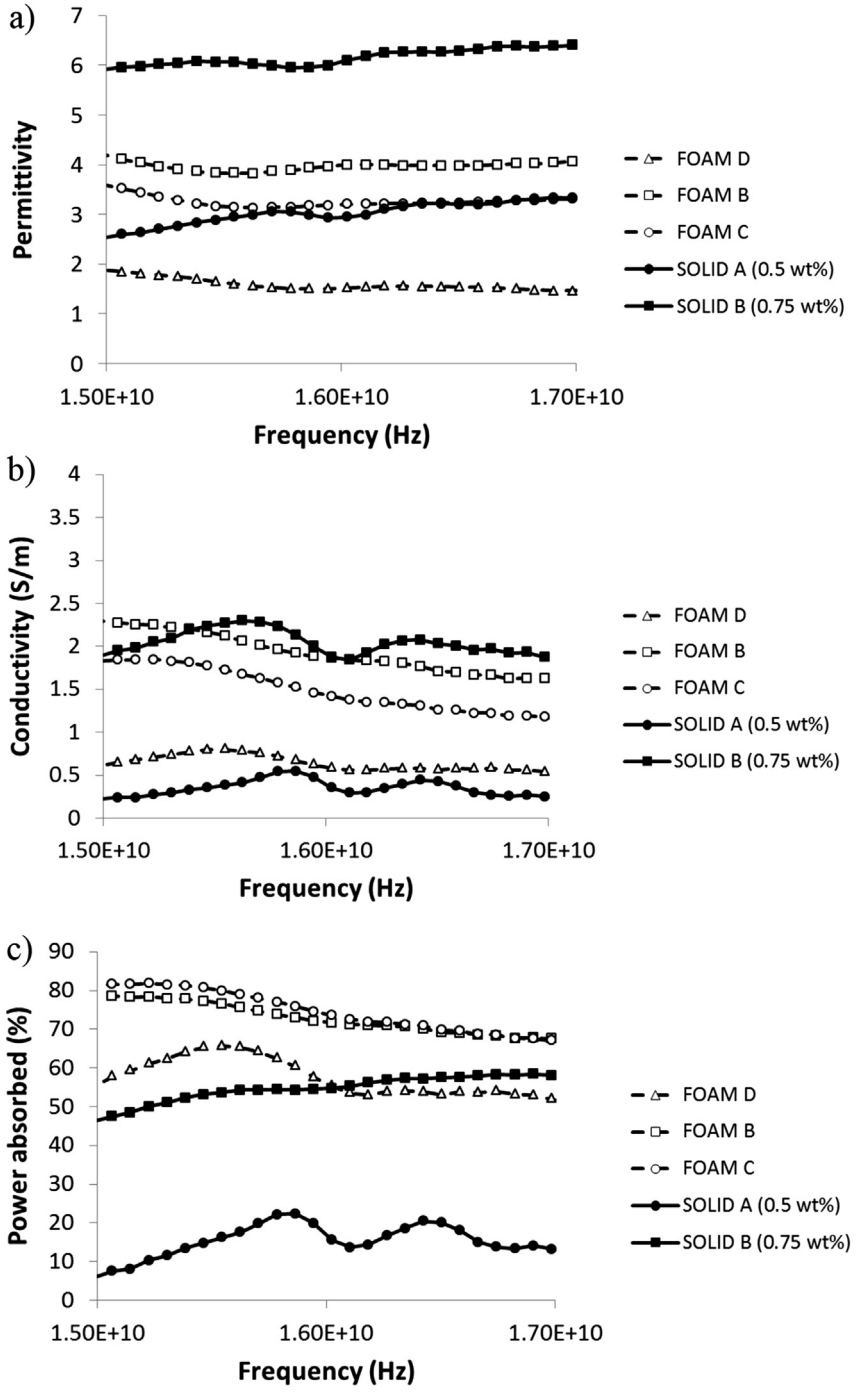

Fig. 14. a) Permittivity, b) conductivity and c) power absorbed of different PC samples.

kept quite low to avoid PC crystallization, the absorbed amount of CO_2 remains low and consequently, the expansion of the nanocomposite during foaming is limited. An increase of the foaming temperature from 190 °C to 200 °C allows to reduce the density of PC/2 wt% MWNTs foams to 0.44 (Table 5). At these values of density, a significant improvement of the EMI absorption is expected and will be quantified in the next section.

3.6. Conductivity performances

The EMI shielding properties of the PC foams has been compared to the solid samples in order to confirm the beneficial effect of foaming. Indeed, the introduction of air upon foaming allows to reduce the permittivity of the samples while the reduction in conductivity is limited. Consequently, a higher permittivity/conductivity ratio can be achieved which is favourable to a high EMI absorption since the reflectivity and the absorption are proportional to the permittivity and the conductivity, respectively. Fig. 14 a and b show that the decrease in samples density upon foaming induces a decrease of both the permittivity and the conductivity. The decrease in electrical conductivity can be explained by the dilution of MWNTs content in volume. However the permittivity is decreasing much faster than the electrical conductivity as can be demonstrated by the comparison with solid samples. Indeed, as illustrated in Fig. 14, foam C has similar permittivity than a solid samples containing 0.5 wt% of CNTs (solid A) but presents a much higher conductivity. Similarly, foam B has a similar conductivity than a solid samples containing 0.75 wt% of CNTs (solid B) but a much lower permittivity. As the result of their improved permittivity/conductivity ratios, the different foams develop much higher absorption properties (above 70%) than the solid samples (below 60%) (Fig. 14c).

4. Conclusions

Blends of polycarbonate (PC) and MWNTs of different compositions, in the form of slabs obtained by melt-extrusion and compression, have been examined by transmission electron microscopy (TEM), rheology, differential scanning calorimetry (DSC) and dynamic mechanical thermal analysis (DMTA). The carbon nanotubes were well-dispersed in the polycarbonate matrix, no agglomeration being observed by TEM analysis, and the percolation threshold was obtained with a minimal proportion of 0.5 wt% MWNTs. After several unsuccessful attempts to obtain well-expansed foams of nanocomposites by treatment with supercritical CO_2, the PC/MWNTs were thermally characterized. The DSC analyses of PC-MWNTs blends show that melting and glass transition temperatures of the components were slightly affected by MWNTs loading, but crystallization of PC was observed, with a maximal degree of crystallinity of 20%. The crystallization of polycarbonate was mainly induced by supercritical CO_2, and a synergic effect was detected with an increasing loading of MWNTs. The dynamic mechanical behaviour of the blends was evidencing the presence of small crystallites, in agreement with the DSC results. This polymer matrix crystallization restricts in an important manner the possibility to produce polycarbonate-based foams of low density and restrains the pressure-temperature window that can be used to generate well-expanded foams by the supercritical CO_2 technology. By using appropriate foaming conditions, PC/MWNTs nanocomposite foams of density around 0.44 g/cm^3 have been prepared. The presence of air within these composite foams allows to improve their permittivity/conductivity ratios, and consequently their ability to absorb EMI radiations. Absorption performances as high as 80% were obtained for the foams compared to maximum 60% for the unfoamed nanocomposites.

Acknowledgements

CERM are grateful to the Région Wallonne for financial support in the frame of the “nanotechnology” program MULTIMASEC. The authors are indebted to the University of Liège and to the National Funds for Scientific Research (F.R.S-FNRS). C.D. and I. H. are “F.R.S-FNRS Research Director” and J.-M. T. is “F.R.S-FNRS logistics collaborator” for the National Funds for Scientific Research (F.R.S-FNRS). The help of Mr David Spote for the electromagnetic measurement setup is also acknowledged.

References

[1] Grady BP. J Polym Sci Part B Polym Phys 2012;50:591–623.
[2] Qian H, Greenhalgh ES, Shaffer MSP, Bismarck A. J Mater Chem 2010;20:4751.
[3] Saib A, Bednarz L, Daussin R, Bailly C, Lou X, Thomassin JM, et al. IEEE Trans Microw Theory Tech 2006;54:2745–54.
[4] Fujigaya T, Nakasima N. J Nanosci Nanotechnol 2012;12:1717–38.
[5] Huang YQ, Wong CKC, Zheng JS, Bouwman H, Barra R, Wahlström B, et al. Environ Int 2012;42:91–9.
[6] Guo J, Liu Y, Prada-Silvy R, Tan Y, Azad S, Krause B, et al. J Polym Sci Part B Polym Phys 2014;52:73–83.
[7] Göldel A, Kasaliwal GR, Pötschke P, Heinrich G. Polymer 2012;53:411–21.
[8] Castillo FY, Socher R, Krause B, Headrick R, Grady BP, Prada-Silvy R, et al. Polymer 2011;52:3835–45.
[9] Wang M, Li B, Wang J, Bai P. Polym Adv Technol 2011;22:1738–46.
[10] Abbasi S, Carreau P, Derdouri A, Moan M. Rheol Acta 2009;48:943–59.
[11] Hornbostel B, Pötschke P, Kotz J, Roth S. Phys E 2008;40:2434–9.
[12] Fornes TD, Baur JW, Sabba Y, Thomas EL. Polymer 2006;47:1704–14.
[13] Chen L, Pang X-J, Yu Z-L. Mater Sci Eng 2007;457:287–91.
[14] Takahashi T, Higuchi A, Awano H, Yonetake K, Kikuchi T. Polym J 2005;37:887–93.
[15] Pötschke P, Abdel-Goad M, Alig I, Dudkin S, Lellinger D. Polymer 2004;45:8863–70.
[16] Thomassin JM, Pagnoulle C, Bednarz L, Huynen I, Detrembleur C. J Mater Chem 2008;18:792–6.
[17] Peng J, Turng L-S, Peng X-F. Polym Eng Sci 2012;52:1463–73.
[18] Seo J-H, Ohm W-S, Cho S-H, Cha SW. Polym-Plast Tech Eng 2011;50:1399–404.
[19] Weller JE, Kumar V. Polym Eng Sci 2010;50:2160–9.
[20] Seo J-H, Cha SW, Kim HB. Polym-Plast Tech Eng 2009;48:351–8.
[21] Fukasawa Y, Chen J, Saito H. J Polym Sci Part B Polym Phys 2008;46:843–6.
[22] Ito Y, Yamashita M, Okamoto M. Macromol Mater Eng 2006;291:773–83.
[23] Gross SM, Roberts GW, Kiserow DJ, DeSimone JM. Macromolecules 2000;33:40–5.
[24] Kumar V, Suh NP. Polym Eng Sci 1990;30:1323–9.
[25] Coleman JN, Khan U, Blau WJ, Gun'ko YK. Carbon 2006;44:1624–52.
[26] Coleman JN, Khan U, Gun'ko YK. Adv Mater 2006;18:689–706.
[27] Alig I, Lellinger D, Engel M, Skipa T, Poetschke P. Polymer 2008;49:1902–9.
[28] Moon SI, Jin F, Lee CJ, Tsutsumi S, Hyon SH. Macromol Symp 2005;224:287–95.
[29] Donald K, White RJ. A handbook on electromagnetic shielding materials and performances. USA: Library of Congress; 1975.
[30] Okatomo KT. Microcellular processing. Munich: Hanser Publishers; 2003.
[31] Bledzki AK, Rohleder M, Kirschling H, Chate A. J Cell Plast 2010;46.
[32] Wolff F, Zirkel L, Betzold S, Jakob M, Maier V, Nachtrab F, et al. Int Polym Process 2011;26:437–43.
[33] Xu Z-M, Jiang X-L, Hu G-H, Zhao L, Zhu Z-N, Yuan W-K. J Supercrit Fluids 2007;41:299–310.
[34] Ramesh NS, Rasmussen DH, Campbell GA. Polym Eng Sci 1994;34:1685–97.
[35] Ramesh NS, Rasmussen DH, Campbell GA. Polym Eng Sci 1994;34:1699–706.
[36] Chiou JS, Barlow JW, Paul DR. J Appl Polym Sci 1985;30:2633–42.
[37] Shieh Y-T, Su J-H, Manivannan G, Lee PHC, Sawan SP, Spall WD. J Appl Polym Sci 1996;59:707–17.
[38] Zhang Z, Handa PY. J Polym Sci Part B Polym Phys 1998;36:977–82.
[39] Bos A, Pünt IGM, Wessling M, Strathmann H. J Membr Sci 1999;155:67–78.
[40] Alessi P, Cortesi A, Kikic I, Vecchione F. J Appl Polym Sci 2003;88:2189–93.
[41] Kusmanto F, Billham M, Hornsby P. J Vinyl Addit Technol 2008;14:163–6.
[42] Alizadeh A, Sohn S, Quinn J, Marand H, Shank LC, Iler HD. Macromolecules 2001;34:4066–78.
[43] Chiou JS, Barlow JW, Paul DR. J Appl Polym Sci 1985;30:3911–24.
[44] Mizoguchi K, Hirose T, Naito Y, Kamiya Y. Polymer 1987;28:1298–302.
[45] Beckman E, Porter RS. J Polym Sci Part B Polym Phys 1987;25:1511–7.
[46] Handa PY, Zhang Z, Roovers J. J Polym Sci Part B Polym Phys 2001;39:1505–12.
[47] Takada M, Hasewaga S, Oshima M. Polym Eng Sci 2004;44:186–96.
[48] Tomasko DL, Li H, Liu D, Han X, Wingert MJ, Lee LJ, et al. Ind Eng Chem Res 2003;42:6431–56.
[49] Mascia L, Del Re G, Ponti PP, Bologna S, Di Giacomo G, Haworth B. Adv Polym Technol 2006;25:225–35.
[50] Liao X, Wang J, Li G, He J. J Polym Sci Part B Polym Phys 2004;42:280–5.

[51] Mercier JP, Legras R. J Polym Sci Polym Lett Ed 1970;8:645–50.
[52] Zhai W, Yu J, Ma W, He J. Macromolecules 2007;40:73–80.
[53] Hu X, Lesser AJ. Polymer 2004;45:2333–40.
[54] Legras R, Mercier JP, Nield E. Nature 1983;304:432.
[55] Di Maio E, Iannace S, Sorrentino L, Nicolais L. Polymer 2004;45:8893–900.
[56] Lopez-Periago A, Garcia-Gonzalez A, Domingo C. J Appl Polym Sci 2009;111:291–300.
[57] Jonza JM, Porter RS. J Polym Sci Part B Polym Phys 1986;24:2459–72.
[58] Kambour RP, Karasz FE, Daane JH. J Polym Sci Part A-2 1966;4:327–47.
[59] Turska E, Benecki W. J Appl Polym Sci 1979;23:3483–500.
[60] Zhai W, Yu J, Weiming M, He J. Polym Eng Sci; 2007:1338–43.
[61] Ware RA, Tirtowidjojo S, Cohen C. J Appl Polym Sci 1981;26:2975–88.
[62] Sundararajan PR, Singh S, Moniruzzaman M. Macromolecules 2004;37:10208–11.
[63] Tsuburaya M, Saito H. Polymer 2004;45:1027–32.
[64] Marrazzo C, Di Maio E, Iannace S. Polym Eng Sci 2008;48:336–44.
[65] Sung YT, Kum CK, Lee HS, Byon NS, Yoon HG, Kim WN. Polymer 2005;46:5656–61.
[66] Urbanczyk L, Calberg C, Detrembleur C, Jérôme C, Alexandre M. Polymer 2010;51:3520–31.
[67] Cao X, Lee LJ, Widya T, Macosko C. Polym-Plast Tech Eng 2005;46:775–83.
[68] Wong A, Park CB. Chem Eng Sci 2012;75:49–62.
[69] Wu S, Liu X, Yeung KWK, Hu T, Xu Z, Chung JCY, et al. Acta Biomater 2011;7:1387–97.
[70] Quiévy N, Bollen P, Thomassin J-M, Detrembleur C, Pardoen T, Bailly C, et al. Electromagnetic absorption properties of carbon nanotube nanocomposite foam filling honeycomb waveguide structures. IEEE Trans Electromagn Compat (Special Issue on Nanotechnology);54(1):43–51.